Ab initio investigation of the nitrofluoride SiNF

Emmanuel Betranhandy, Samir F. Matar

Ab initio investigation of the nitrofluoride SiNF

E. Betranhandy and S. F. Matar*
Institut de Chimie de la Matière Condensée de Bordeaux CNRS, Université Bordeaux 1, 87 Avenue du Dr. Albert Schweitzer, F-33608 Pessac Cedex, France

(Received 6 June 2005; revised manuscript received 30 June 2005; published 7 November 2005)

A new chemical system SiNF is proposed as a candidate for potential applications based on calculations within the density functional theory in its local density approximation. Different structural setups were built based on a geomimetism principle. All proposed structures were fully geometry optimized using ultrasoft pseudopotentials. From the cohesive energies used as a selection criterion TiOCl-derived and stishovite-based silicon nitrofluoride are evidenced as most stable varieties. The electronic band structure and chemical bonding properties show insulating behavior with a wide band direct gap and stress the different chemical roles played by nitrogen and fluorine. Theoretical *K*-edge XANES spectra for Si, N, and F are provided as a signature tool of analysis for potential syntheses.

DOI: 10.1103/PhysRevB.72.205108 PACS number(s): 71.15.Mb, 61.50.Ah

I. INTRODUCTION

The properties (whether they are nano-, micro-, or macroscopic) of a material are due to its formulation and nature of the chemical interactions between its constituents as well as to its shaping. One of the best examples is the research on ultrahard materials, in which strong covalency and a tridimensionality (due to sp^3 hybridization) are priviledged in order to provide an improved resistance against lattice deformations.[1,2] In the mixed-anions materials, both ionic and covalent bonds are present, and are expected to induce a specific dimensionality as well as interesting new properties.

As in the case study of ultrahard materials, for which boron, carbon, and nitrogen light elements were selected to provide the bases for new formulations and structures, new stoichiometries for mixed-anions compounds can be defined. Considering that the isoelectronicity rule for valence shell states whereby 2O $(2s^2,2p^4)$=N $(2s^2,2p^3)$+F $(2s^2,2p^5)$, nitrofluorides of formulation A^{IV} NF type can be proposed as isoelectronic of $A^{IV}O_2$, where A^{IV} is a generic tetravalent element. A^{IV} is likely to form covalent bonds with nitrogen, while fluorine is expected to form ionic bonds. We can notice the existence of crystalline Ca_2NF,[3] Mg_2NF (with H or another ligand inside)[4] or ZrNF,[5] which are isoelectronics of the oxides CaO (for 2 formula units—f.u.), MgO (for 2 f.u.), and ZrO_2, respectively. These oxides are known to present an ionic character of the metal-oxygen bonds.[6] Moreover, considering that at room temperature and pressure, the lightest element which produces a solid $A^{IV}O_2$ is silicon for the α quartz (SiO_2), SiNF stoichiometry appears to be a good and new candidate as a mixed-anions compound. As a consequence, properties such as a anisotropic electric conduction or optical anistropy can be sought, as well as its growth in thin films or at nanoscopic scales.

The starting model structures were built based on a principle which mimics known mineral structures. We call this "geomimetism" (as derived from biomimetism), which consists here in selectively substituting chemical species by other ones, namely silicon, nitrogen, and fluorine. As an application of the geomimetism principle, first results[7] on relative stability for SiNF were obtained from SiO_2 and from pyrite and fluorite derived structures. The most stable polymorph was found to be stishovite-based SiNF (Fig. 1). Knowing that stishovite is the most unstable SiO_2 polymorph (α quartz being the most stable) one can assign the apparent discrepancy to the opposite chemical roles played by N and F as with respect to the oxide homologous system, although they are isoelectronic. We here analyze such effects where we propose new model crystal structures for SiNF based on binary AX_2 and ternary AXY derived structural types from which we identify the most stable polymorph through geometry optimization. Subsequent analyses of the electronic structure and chemical bonding properties are carried out to assign a role for each constituent in the physical properties. For enforcing the results and in order to give more information for possible syntheses, theoretical x-ray absorption near-edge spectra (XANES) at the *K*-edge are proposed as well.

II. COMPUTATIONAL DETAILS

Two computational methods built within the density-functional theory[8] (DFT) were used, namely, the pseudopotentials VASP package[9] for the geometry optimization and the all electrons augmented spherical wave method[10] (ASW) for an account of the electronic structure (density of states, band structure, and chemical bonding analysis). Within the VASP code, the ion-electron interactions are treated by the ultrasoft pseudopotentials according to Vanderbilt,[11] whereas the electron-electron interaction is described in the local density approximation (LDA) to the DFT by the Ceperley-Alder exchange-correlation potential.[12] In the plane wave pseudopotential approach, the rapid variation of the potential near the nuclei is avoided by substituting the all electrons Hamiltonian with a smoother pseudo-Hamiltonian which reproduces the valence energy spectrum. As a matter of fact, the use of pseudopotentials allows a considerable reduction of the necessary number of plane waves per atom for transition metal and first row elements; thus force and full stress tensor can be easily calculated and used to relax atoms into their ground state. The conjugate-gradient algorithm[13] is used in

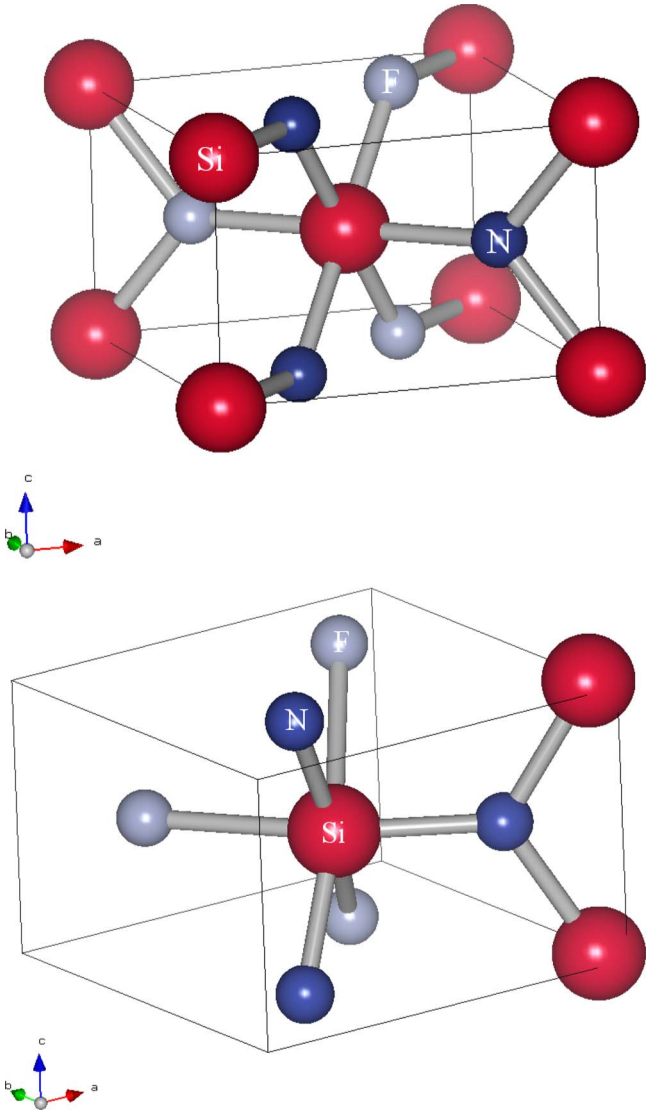

FIG. 1. (Color online) Crystal structures of (a) host undistorted stishovite-like SiNF and (b) relaxed stishovite-like SiNF. Notice the modification in the environment of silicon at center of the cell.

this computational scheme to relax the ions of the different structural setups of SiNF phases. The calculations were performed by using an energy cutoff of 434.8 eV for the plane-wave basis set. The tetrahedron method with Blöchl corrections[14] as well as a Methfessel-Paxton[15] scheme for conducting systems was applied for both geometry relaxation and total energy calculations. Brillouin-zone integrals were approximated using the special *k*-point sampling of Monkhorst and Pack.[16] A large number of 150 *k* points were used in the irreducible wedges of the respective Brillouin zones to perform total energy calculations. The optimization of the structural parameters was performed until the forces on the atoms were less than 0.02 eV/Å and all stress components were less than 0.003 eV/Å^3. In as far as the minimization and/or stabilization energies of the different structures were obtained for the same chemical system SiNF, the energy magnitudes can be compared together for 1 f.u. This corresponds to the cohesive energies: $E_{coh}=E_{min}-E_{atm}$. Here E_{atm} is provided by $Si_{(s)}$, $\frac{1}{2}N_{2(g)}$ and $\frac{1}{2}F_{2(g)}$. As a consequence, we have also calculated E_{coh} besides the minimization energies.

In order to complete the obtained results by an insight on electronic behaviors, the ASW method (Ref. 10) is used. It is based on the atomic sphere approximation (ASA), a special form of muffin-tin approximation which consists in dividing the cell volume into atomic spheres whose total volume is equal to the cell volume. The calculation being carried out in the atomic spheres space, empty spheres (pseudoatoms) need to be introduced in low compactness structures such as those for the systems studied here. In the context of this study, ASW is used (in DFT-LDA) in order to obtain a description of the electronic structure [density of states (DOS) and band structure] on the one hand, and of the chemical bonding on the other hand. Information about the nature of the interaction between atomic constituents can be provided using overlap population (OP) leading to the so-called COOP (crystal orbital overlap population)[17] or alternatively introducing the Hamiltonian based population COHP (crystal orbital Hamiltonian population).[18] Both approaches lead to a qualitative description of the chemical interactions between two atomic species by assigning a bonding, nonbonding, or antibonding character. A slight refinement of the COHP was recently proposed in form of the "covalent bond energy" ECOV which combines both COHP and COOP so as to make the resulting quantity independent of the choice of the zero of potential.[19] The ECOV was recently implemented within the ASW method.[20] Our experience with both COOP and ECOV shows that they give similar general trends although COOP exagerate the magnitude of antibonding states. We shall be using the ECOV description of the chemical bonding.

Further information is brought by the calculation of theoretical XANES carried out with the FDMNES code.[21] A *K*-edge spectrum was calculated for each atomic species within the finite-difference method, chosen for using the LDA in order to avoid the muffin-tin approximation, and as a consequence, to reduce the needed number of parameters which have to be considered without losing precision. Spectra are plotted for the (−5 eV; 50 eV) photon energy range, with a 0.5 eV step, where 0 corresponds to the *K* edge of the considered element: 409.9 eV for nitrogen, 696.7 eV for fluorine, and 1839 eV for silicon. We have chosen an aggregate radius of 4.0 Å, which corresponds to a sphere centered on the absorbing atom wherein final states are calculated. The atoms located out of this sphere are not taken in account for the calculation. Note that every spectrum is a weighted sum of directional (polarized) spectra.

III. CHOICE OF NEW POTENTIAL STRUCTURES

As a preliminary step we have computed the energies of the constituent elements in their stable state, i.e., for diamondlike silicon crystal, for gaseous nitrogen N_2, and gaseous fluorine F_2. For the the two latter, very large cells of 10 Å were used as a simulation box.[9] The obtained energies (per atom) were as follows: $Si_{(s)}$:−5.97 eV, $N_{2(g)}$:−8.50 eV, and $F_{2(g)}$:−2.11 eV. These values will be used to extract the

cohesive energies of the different SiNF varieties: $E_{coh}=E_{min}-E_{atm}$.

From a former work[7] the starting structural setups were selected based on the geomimetism principle presented above. This led us to consider the different varieties of SiO_2 together with pyrite (FeS_2) and fluorite (CaF_2). Consequently we suggest that a protocol be followed, should one propose new stoichiometries, is to start from isoelectronicity rules [e.g., 2C $(2s^2,2p^2)$=N $(2s^2,2p^3)$+B $(2s^2,2p^1)$ or as it is proposed here, 2O=N+F] and then to suggest candidate host structures. Due to the different chemical nature of the atoms one expects modifications from subsequent geometry optimization (see Figs. 1 and 2). The major outcome of the geometry optimizations was the anisotropy for the atomic positions and lattice distortions. This result should be assigned to the different chemical natures of N and F. From this new potential structures can be selected from those allowing for arrays of atoms to develop in selective directions such as the quasi-two-dimensional crystal systems AlB_2 and CdI_2 types as well as pseudolayered ternaries such as PbFCl and TiOCl. While the geomimetism criterion is applied as before, we here go beyond the isoelectronicity criterion which was used to postulate SiNF.[7] Both AlB_2 and CdI_2 can be presented as AX_2 hexagonal crystal structures wherein A atoms form successive parallel planes between which the X_2 entity is inserted. The difference is in their respective X_2 orientation: parallel to the "A" plane in the AlB_2 case, but not in the CdI_2 case. A difference between relative stabilities is then expected, as a consequence of new substructures induced by the X pair substitution. In the case of ternaries, the interest is in the consequences of the anionic substitutions. Their compositions involve differences in atomic volumes repartition ($V_{Pb} \gg V_F$) or in charge distribution in crystal cell.

A. Model structures based on AX_2 binary systems AlB_2 and CdI_2

AlB_2 is a one formula unit (f.u.) hexagonal structure with $P6/mmm$ space group (No. 191): Al($1a$) at (0 0 0), whereas B($2d$) at $(\frac{1}{3}\ \frac{2}{3}\ \frac{1}{2})$ and $(\frac{2}{3}\ \frac{1}{3}\ \frac{1}{2})$ forms graphitelike planar sheets. The derived model structure is based on a substitution of Al by Si, on the one hand, and of a substitution of B by N and F on the other hand thus leading to one SiNF f.u.. One can remark that there is a single possible anionic substitution which leads to create an electric dipole. After geometry optimization, the obtained structure keeps the hexagonal symmetry (a=3.741 Å, c=2.290 Å, V=27.77 Å^3/f.u.) but the final space group is now $P\bar{6}m2$ (No. 187) with the same positions of all species: Si($1a$), N($1d$), F($1f$). The reached minimization energy is −14.916 eV/f.u., which classifies this model structure as quite unstable, compared with the other ones[7] (cf. Table I).

CdI_2 (one f.u.) is a hexagonal phase which belongs to the $P\bar{3}m1$ space group (No. 164): Cd($1a$) at (0 0 0) and I($2d$) at $(\frac{1}{3}\ \frac{2}{3}\ \frac{1}{4})$ and $(\frac{2}{3}\ \frac{1}{3}\ \frac{3}{4})$. As previously noticed, the main difference between CdI_2 and AlB_2 is in the position of the anionic pair with respect to the A plane, and, as for AlB_2, the derived model structure is based on a Cd substitution by Si, on the one hand, and of iodine substitution by N and F. Here also there is a single possible anionic substitution which leads to create a dipole. The optimized model structure is kept hexagonal (a=2.810 Å, c=4.605 Å, V=31.50 Å^3/f.u.), but the atomic positions have changed with respect to the initial geometry. The new space group is $P3m1$ (No. 156), where Si is in a ($1a$) site with z=0, N in a ($1b$) site with z=0.1140 and F in a ($1c$) site with z=0.7053. The reached minimization energy is −22.216 eV/f.u.: the considered structure is one of the most stable calculated ones (cf. Table I).

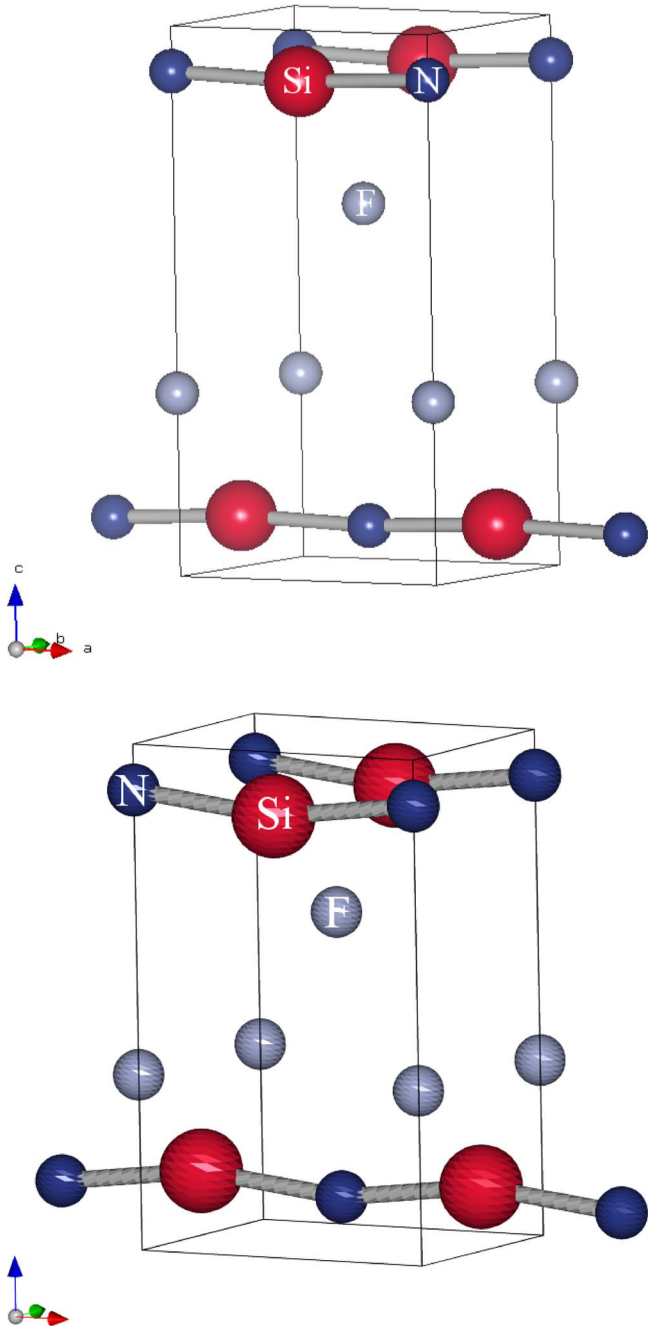

FIG. 2. (Color online) Crystal structures of (a) host undistorted TiOCl-like SiNF and (b) relaxed TiOCl-like SiNF.

A relevant remark concerning AlB_2-derived SiNF is in a second optimization carried out with N and F atoms posi-

TABLE I. Summary of results on SiNF theoretical structures, classified according to their relative stabilities. Indicated atom-atom distances correspond to the lowest measured value (first neighbor of a defined species).

Model structure	E/f.u. (eV)	V/f.u. (Å^3)	$d_{Si—N}$ (Å)	$d_{Si—F}$ (Å)	$d_{N—F}$ (Å)	E_{coh} (kJ/mol)
SiNF(TiOCl)	−22.642	28.06	1.798	1.860	2.480	−585.8
SiNF(stishovite) (Ref. 7)	−22.442	27.04	1.697	2.173	2.567	−566.5
SiNF(CdI_2)	−22.216	31.50	1.703	2.115	2.484	−544.7
SiNF(PbFCl)	−19.672	26.80	1.747	1.779	2.437	−299.3
SiNF(AlB_2)	−14.916	27.77	2.445	2.445	2.160	159.6

tioned as follows: $N(\frac{1}{3}\ \frac{2}{3}\ \frac{1}{2}-\delta)$ and $F(\frac{2}{3}\ \frac{1}{3}\ \frac{1}{2}+\delta)$ with $0<\delta<\frac{1}{2}$, i.e., with atoms put off the graphiticlike plane. The resulting structures are the same as previously described for a geometry-optimized CdI_2 derived SiNF. This shows that AlB_2-derived SiNF is likely to be a metastable system compared to the CdI_2-derived one.

B. Model structures based on *AXY* ternary systems PbFCl and TiOCl

PbFCl is tetragonal with two f.u. per unit cell within the $P4/nmm$ space group (No. 129) where F is in a ($2a$) site, Pb and Cl in ($2c$) sites, whereas TiOCl is orthorhombic ($Pmmn$ space group No. 59) and can be considered as a distortion of the PbFCl structure. Titanium atoms are in ($2b$) sites whereas oxygen and chlorine atoms are in ($2a$) sites. In the case of PbFCl three selective substitutions were carried out because Pb and Cl are in the same Wyckoff crystallographic sites allowed by the sructure. From preliminary tests of substitutions within the starting lattice and subsequent geometry optimizations, the most stable structure is found by preserving the original site of F while Si and N substitute for Pb and Cl. The characteristics of the resulting crystal is such as: space group $P4mm$ (No. 99), $a=b=2.811$ Å, $c=6.781$ Å, $V=26.80$ Å^3/f.u.; Si1 ($1a$) at (0 0 0), Si2 ($1b$) at $(\frac{1}{2}\ \frac{1}{2}\ 0.6105)$, N1 ($1a$) at (0 0 0.5677), N2 ($1b$) at $(\frac{1}{2}\ \frac{1}{2}\ 0.8674)$, F($2c$) at $[(\frac{1}{2}\ 0\ 0.1609), (0\ \frac{1}{2}\ 0.1609)]$ with $E=-19.672$ eV/f.u..

Considering the TiOCl structure type, three substitutional schemes were envisaged due to the fact that O and Cl are in the same type of crystallographic sites allowed in the structure. The results of geometry optimizations point to the most stable structure as corresponding to Si(Ti), N(O) and F(Cl) substitutions. The crystal structure characteristics are space group $P3mmn$ (No. 59) $a=2.761$ Å, $b=3.573$ Å, $c=6.688$ Å, $V=28.065$ Å^3/f.u.; Si($2a$) at $(\frac{1}{4}\ \frac{1}{4}\ 0.1263)$, N($2b$) at $(\frac{1}{4}\ \frac{3}{4}\ 0.0907)$, F($2b$) at $(\frac{1}{4}\frac{3}{4}\ 0.6536)$ with $E=-22.641$ eV/f.u.

The numerical results are shown in Table I in which data on stishovite-derived SiNF from a former investigation[7] are added for sake of comparison. All structures except for the AlB_2-derived structure are expectedly, i.e., from chemical bonding and electrostatic repulsion criteria, characterized by shorter Si—N ($1.7<d_{Si—N}<1.8$ Å) than Si—F distances ($1.8<d_{Si—N}<2.18$ Å) and a long N—F separation ($d_{Si—N}=2.5$ Å). They possess similar energy magnitudes per f.u. with a TiOCl based system found to be most stable. Its crystal structure is shown in Fig. 2 which can be considered along the vertical axis as a stacking of Si—N planes interlayered by F ones and illustrates the numerical results. The AlB_2-type SiNF which is found the most unstable exhibits longer Si—N/Si—F distances as with respect to N—F. Further illustration will be obtained from the assessment of electronic structure and chemical bonding criteria presented hereafter for the most stable SiNF polymorph.

IV. ELECTRONIC PROPERTIES OF TiOCl-DERIVED SINF

The computation of the electronic properties was carried out by use of all electron ASW method for analyzing the site projected DOS as well as the chemical bonding. Within the ASA approximation empty spheres (ES) were introduced. At self-consistent convergence, charge transfer was observed to be from Si ($\Delta Q\sim-2.9$) and N ($\Delta Q\sim-0.7$) to ES, with little charge transfer for F. While such values are to be considered qualitatively in as far the choice of the sphere radii is not unique in the ASA; this could point to a covalent behavior within the Si/N sublattice as opposed to the fluorine one. Nevertheless the amount of charge transfer does not translate an ionic behavior (such as Si^{4+}, N^{3-}, F^-) rarely observed in

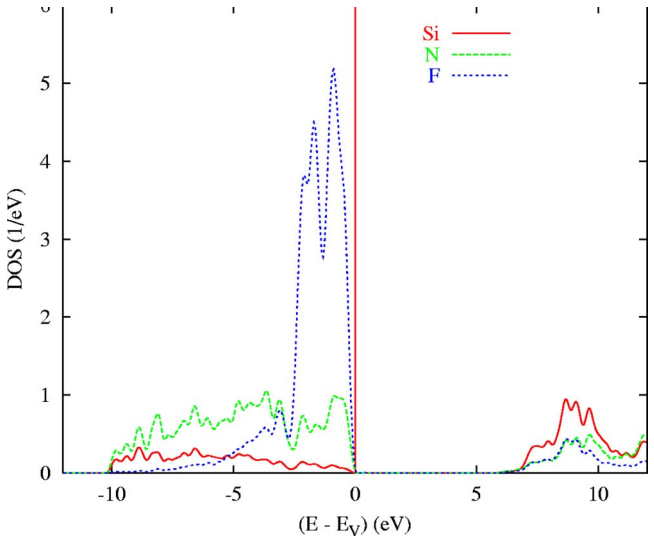

FIG. 3. (Color online) Site projected DOS for TiOCl-derived SiNF.

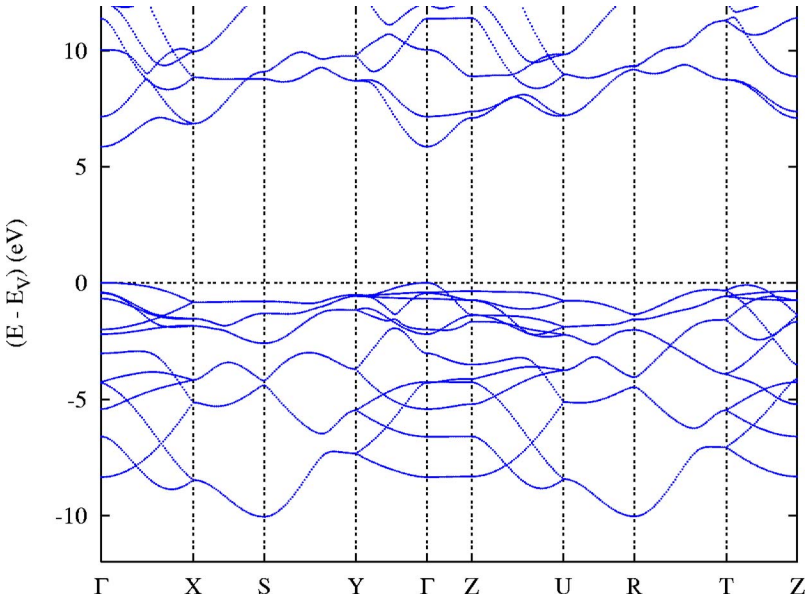

FIG. 4. (Color online) Band structure for TiOCl-derived SiNF.

the framework of such calculations. A more meaningful picture is provided from the quantum mixing of the valence states as it is shown by the plot of the site projected DOS given in Fig. 3. Energy reference is taken with respect to the top of the valence band (VB). Localized low-lying F($2s$) states are not shown here: this allows us to focus on the analysis on the p-states mixing between the relevant chemical species within the VB. The system is found to be an insulator with a relatively wide gap of ~6 eV, while stishovite-derived SiNF is a semiconductor with a ~0.7 eV gap.[7] The discrepancy is likely related with the layer-like lattice of TiOCl as opposed to 3D stishovite whereby a larger ionic character is allowed for in the former (cf. Fig. 1). From the band structure presented in Fig. 4, the gap is found directly between Γ_{VB} and Γ_{CB}; the flat band behavior arising from F states around the top of the VB is opposed to the relatively dispersed bands between −10 and −4 eV, mainly due to mixing between Si and N states as observed with the DOS at the lower part of the VB, where Si and N DOS follow similar skylines, while this is totally modified at the top of VB where F states are dominant.

The pair interactions based on ECOV criterion of chemical bonding are plotted in Fig. 5. The energy reference is taken with respect to the top of the valence band (VB). Negative, positive and zero ECOV magnitudes point to bonding, antibonding, and nonbonding interactions, respectively. Si—N is the main stabilizing interaction all over the VB, while the Si—F bonding occurs around the VB top with much smaller magnitude: this would mean that most of F electrons are nonbonding. Antibonding Si—F states are observed between −1 and 0 eV, which is a consequence of the large filling of F $2p$ states as with respect to N $2p$. Albeit small in magnitude a relevant feature of N—F bonding up −3 eV is observed starting to be antibonding around the top of the VB. From this analysis, it can be pointed out that the SiNF system is stabilized both with Si—N and Si—F inter-

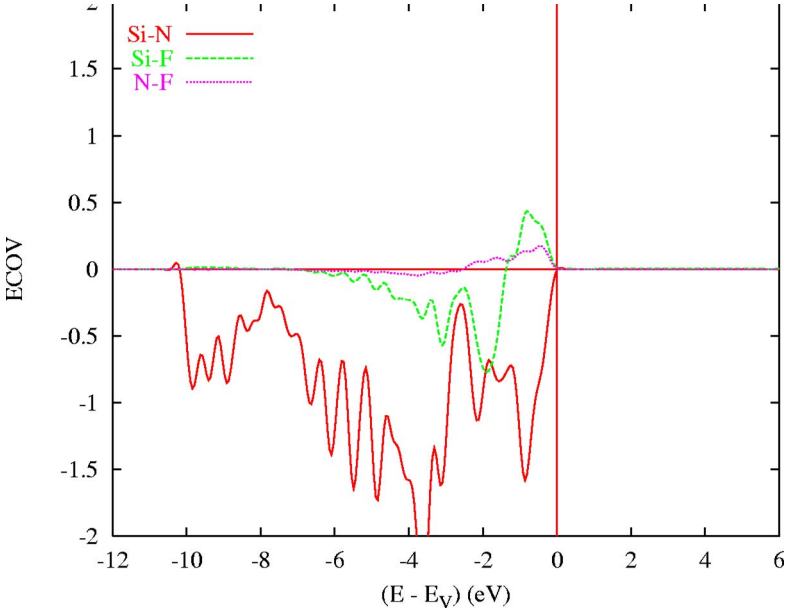

FIG. 5. (Color online) Covalent bond energy for three types of interactions in TiOCl-derived SiNF.

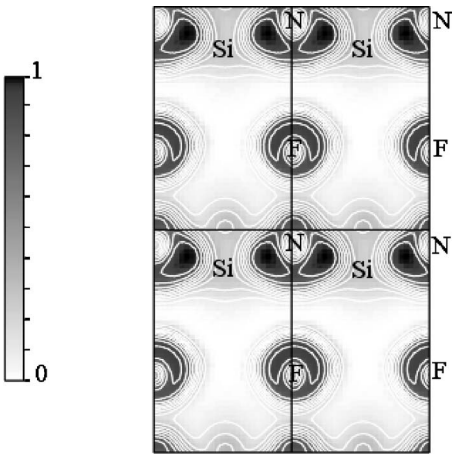

FIG. 6. Electron localization function map of the [010] plane for TiOCl-derived SiNF (substitution type I). Here, four cells (2×2) are represented in each case, and this plane contains—in this figure—the three atomic species Si, N, and F.

actions with a much smaller magnitude for the latter. It can be pointed out that the difference of the bonding of Si toward N and F might explain why fluorine hardly displaces nitrogen in the synthesis routes which are being followed (cf. concluding remarks).

In a second step from which we illustrate electron distribution maps, we focus on the electron localization function[23] (ELF) as obtained from the pseudopotential computations. By this function one seeks the isolocalization surfaces three dimensional (3D) or contour lines (2D section), in order to qualify the chemical interactions. ELF is a normalized function between 0 and 1 where 0 corresponds to nil localization, and 1 to a localization maximum. In order to give a pertinent (but partial) description of the electronic localization in the crystal, an illustration is given in Fig. 6. A high localization (close to 1) between two atoms corresponds to a covalent bond which is well illustrated from the local part of the map showing silicon and nitrogen. This, in connection with the ECOV curve, allows us to confirm the covalent character of Si—N interaction. The half-circle form of the high electron localization indicates a polarization of this bond, which was expected considering the difference of electronegativies[24] between N ($\chi_{Pauling}=3.04$, $\chi_{Allred\text{-}Rochow}=3.07$) and Si ($\chi_P=1.90$, $\chi_{AR}=1.74$).

Quasispherical electron high-localization zones are centred around the fluorine atoms, with slight hornlike deformations which point toward silicon atoms: this confirms the differences of magnitudes between both Si—N and Si—F ECOV plots—i.e., between Si—N and Si—F chemical interactions—and enforces the qualification of ionic bond for the latest one. Concerning the (slightly antibonding) N—F interaction, ELF maps and the consideration of 3D isolocalization surfaces (not presented here) indicate that there is no localization between any fluorine and nitrogen atoms, and, as a consequence no chemical bonding. This seemingly contradicting remark with the ECOV analysis should be connected with a rather electrostatic nature of N—F interaction.

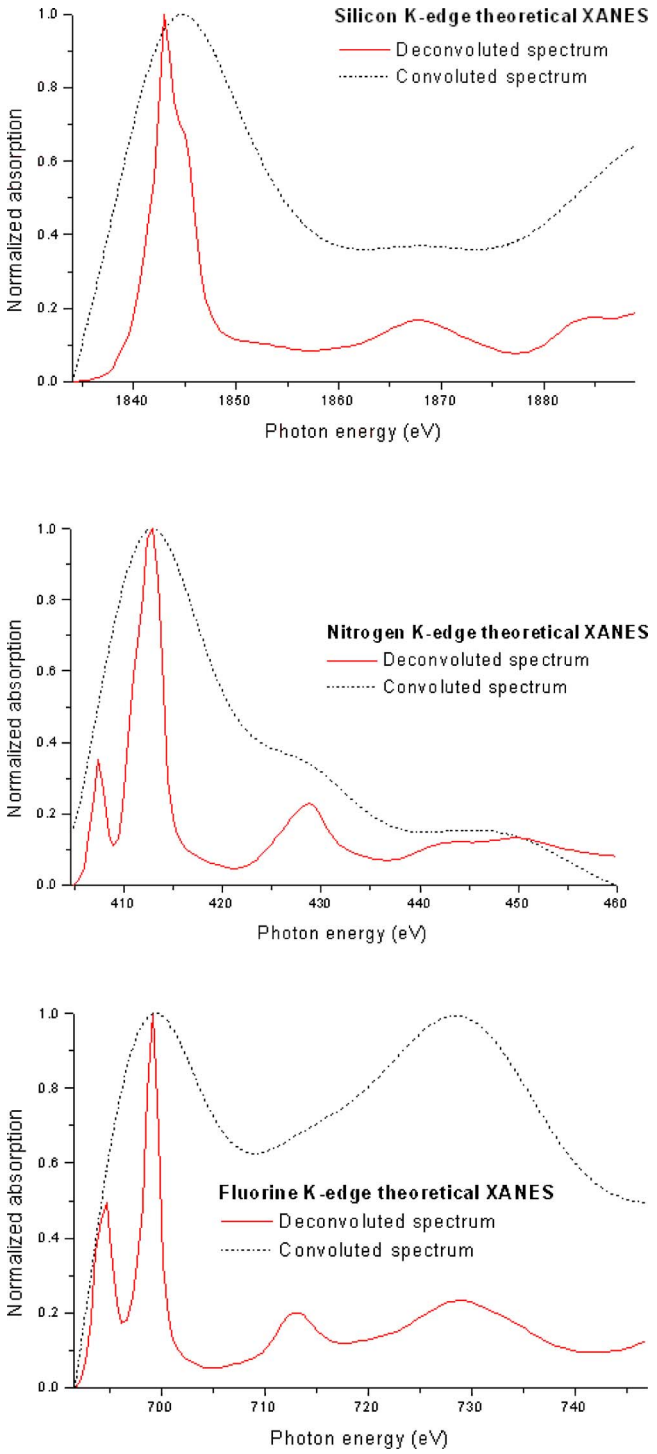

FIG. 7. (Color online) X-ray absorption near-edge spectra of TiOCl-derived SiNF (I), for silicon *K* edge 7(a)-, for nitrogen *K* edge, (b) and fluorine *K* edge, (c)-. Spectra are normalized according the following formula: ($A_{Norm}=[A(E)-A_{min}]/(A_{max}-A_{min})$).

V. THEORETICAL XANES SPECTRA OF TiOCl-DERIVED SINF

XANES is a probe of local chemical environments within a system, i.e., a signature that can be used for analysis in multiphasic compounds. This is especially true when preparation routes of SiNF are being considered either through

solvothermal processes or under gaseous flow with the first results pointing to mixtures of chemical systems.[25,26] The *K*-edge spectra for each considered atomic species (Si, N, and F) are presented in Fig. 7. Mainly for Si *K*-edge and N *K*-edge spectra there is a good agreement with the experimentally obtained XANES patterns for silicon-based compounds such as Si and SiN_x (Refs. 27–29) and SiN_xO_y (Ref. 30) for thin-film samples essentially. However, one can note the maxima peak shifts, which can be attributed to the presence of fluorine: as a matter of fact, an increase of the crystal ionicity shifts these peaks to the higher energies as experimentaly observed for SiN_xO_y with various oxygen rates and with SiO_2 taken as references.

VI. CONCLUDING REMARKS

Based on a geomimetism principle we have proposed a panel of potential theoretical structures for a new nitrofluoride SiNF. From a geometry optimization procedure, it was pointed out to the TiOCl-type–derived system as the most likely stable structure. Its electronic properties show an insulating behavior with a VB dominated with Si—N covalent interaction, while the Si—F ionic bond is less engaged in the bonding. The electron distribution as obtained from ELF plots is another illustration of anisotropic nature of chemical bonding within such a system, which should bring about interesting physicochemical properties. Different preparation routes of SiNF are presently being evaluated, mainly the solvothermal processes[25] on one hand, and reactions under gaseous flows of fluorine or HF (Ref. 26) on the other hand. The preliminary results show the presence of a thin layer of fluorinated silicon on the grains of silicon nitride. This is being analyzed by the x-ray photoemission spectroscopy technique.

ACKNOWLEDGMENTS

One of us (E.B.) acknowledges the Aquitaine Regional Council and the French National Centre of Scientific Research (CNRS) for its financial support, and Dr. Y. Joly for his help on FDMNES. Calculations were done on the Regatta IBM *p690* supercomputer of the "M3PEC-Mésocentre Régional" for intensive numerical computations facility of the University Bordeaux 1, partly financed by the Aquitaine Regional Council.

*Corresponding author: matar@icmcb-bordeaux.cnrs.fr

[1] A. L. Liu and M. L. Cohen, Science **245**, 841 (1989).
[2] E. Betranhandy, S. F. Matar, Ch. El-Kfoury, R. Weihrich, and J. Etourneau, Z. Anorg. Allg. Chem. **630**, 2587 (2004).
[3] R. A. Nicklow, T. R. Wagner, and C. C. Raymond, J. Solid State Chem. **160**, 134 (2001).
[4] S. Andersson, J. Solid State Chem. **1**, 306 (1970).
[5] L. Zhu, X. Chen, and S. Yamanaka, Solid State Commun. **130**, 227 (2004).
[6] J. C. Phillips, *Bonds and Bands in Semi-conductors* (Academic Press, New York, 1973), Chap. 2.
[7] E. Betranhandy, G. Demazeau, and S. F. Matar, Comput. Mater. Sci. **34**, 22 (2005).
[8] W. Kohn and L. J. Sham, Phys. Rev. **140**, A1133 (1965); P. Hohenberg and W. Kohn, Phys. Rev. **136**, B864 (1964).
[9] G. Kresse and J. Hafner, Phys. Rev. B **47**, R558 (1993); G. Kresse and J. Hafner, *ibid.* **49**, 14251 (1994); G. Kresse and J. Furthmüller, Comput. Mater. Sci. **6**, 15 (1996); Phys. Rev. B **54**, 11169 (1996).
[10] A. R. Williams, J. Kübler, and C. D. Gelatt Jr., Phys. Rev. B **19**, 6094 (1979). For a recent review: V. Eyert, in *Electronic Structure of Material*, edited by M. Defranceschi; special issue of Int. J. Quantum Chem. **77**, 1007 (2000).
[11] D. Vanderbilt, Phys. Rev. B **41**, R7892 (1990).
[12] M. Parrinello and A. Rahman, Phys. Rev. Lett. **45**, 1196 (1980).
[13] W. H. Press, B. P. Flannery, S. A. Teukolsky, and W. T. Vetterling, *Numerical Recipes* (Cambridge University Press, New York, 1986).
[14] P. E. Blöchl, O. Jepsen, and O. K. Andersen, Phys. Rev. B **49**, 16223 (1994).
[15] M. Methfessel and A. T. Paxton, Phys. Rev. B **40**, 3616 (1989).
[16] H. J. Monkhorst and J. D. Pack, Phys. Rev. B **13**, 5188 (1976).
[17] R. Hoffmann, Angew. Chem., Int. Ed. Engl. **26**, 846 (1987).
[18] R. Dronskowski and P. E. Blöchl, J. Phys. Chem. **97**, 8617 (1993).
[19] G. Bester and M. Fähnle, J. Phys.: Condens. Matter **13**, 11541 (2001); **13**, 11551 (2001).
[20] V. Eyert and S. F. Matar (unpublished).
[21] Y. Joly, Phys. Rev. B **63**, 125120 (2001).
[22] R. W. G. Wyckoff, *Crystal Structures* (John Wiley & Sons, New York, 1963), Vol. 1, p. 318.
[23] A. D. Becke and K. E. Edgecombe, J. Chem. Phys. **92**, 5397 (1990).
[24] P. Granger, *Panorama des Liaisons Chimiques* (Masson, Paris, 1997), pp. 48–49.
[25] G. Demazeau, J. Mater. Chem. **9**, 15 (1999).
[26] A. Tressaud (private communication).
[27] Joe Wong, Z. U. Rek, M. Rowen, T. Tanaka, F. Schäfers, B. Müller, G. N. George, I. J. Pickering, G. Via, B. DeVries, G. E. Brown, Jr., and M. Fröba, Physica B **208–209**, 220 (1995).
[28] N. Nakamura, K. Hirao, and Y. Yamauchi, Nucl. Instrum. Methods Phys. Res. B **217**, 51 (2004).
[29] J. Tsukajima, K. Arai, S. Takatoh, T. Enokijima, T. Hayashi, T. Yikegaki, A. Kashiwagi, K. Tokunaga, T. Suzuki, T. Fujikawa, and S. Usami, Thin Solid Films **281–282**, 318 (1996).
[30] D. Criado, M. I. Alayo, I. Pereyra, and M. C. A. Fantini, Mater. Sci. Eng., B **112**, 123 (2004).